The Interaction of a Supercritical Fluid Free-Jet Expansion With a Flat Surface

Imane Khalil and David R. Miller*
Dept. of Mechanical and Aerospace Engineering, University of California at San Diego,
La Jolla, California, USA, 92093-0411
* dmiller@ucsd.edu ; fax : 858/534-4543

We report experimental and numerical studies of supersonic free-jet expansions of supercritical CO_2 into atmosphere and impacting on a flat plate, simulating the use of such expansions in thin film growth. We report numerical calculations for the axisymmetric, two-dimensional expansion using a time marching Lax-Wendroff method, incorporating the Redlich-Kwong equation of state to model CO_2. We also compare the quasi-one dimensional gas dynamic approximation for Redlich-Kwong, Peng-Robinson, and ideal gas equations of state. We report experimental data for free-jet expansions of CO_2 from sharp-edged orifices, with diameters D less than 100 micron, source conditions of 70^oC and 8 MPa, and impacting plates at distances from x/D = 5 to 20 nozzle diameters from the source. The data include mass flow rates, optical shadowgraph measurements of the jet and shock wave structure, and impact pressure and temperature measurements along the plate.

INTRODUCTION

There are now several excellent texts summarizing the properties and innovative uses of supercritical fluids SCF [1]. The rapid expansion of supercritical solutions (RESS) has been studied for nearly twenty years since the early papers of Smith and coworkers [2] to growth thin films. In this process, solutes are extracted into a SCF carrier fluid solvent at high pressures but moderate temperatures, and the solution is decompressed in a rapid supersonic free-jet expansion, during which small clusters of solutes may form. The jet is directed at a surface where the solute deposits into thin films of varying morphology [1].

Although the RESS process has been demonstrated to produce a range of particle size and film morphologies, there has been little advancement in quantitative predictions for this complicated process. Not only are the gas dynamics difficult because the fluids are non-ideal and the flows involve shock waves, but the clustering formation kinetics, particle growth in the expansion, and subsequent surface interactions are not understood. Most often quasi-one dimensional (QOD) approximations to the subsonic and supersonic flows are utilized to model the flow field [3-7]. A difficult part of the RESS fluid mechanics is the supersonic free-jet expansion. For ideal gases, there have been several rigorous calculations of axisymmetric free-jet supersonic expansions, which have formed the basis of the use of these expansions for molecular beam research for forty years [8], including the method of characteristics [8,9] and time marching techniques [10,11]. The time marching methods are useful to correctly capture shock wave structure and to include kinetic effects [11,12]. We are not aware of any published three dimensional or axisymmetric calculations for supercritical fluid free-jet expansions incorporating realistic equation of states with both repulsive and attractive corrections to the ideal gas. We begin such an effort by studying free-jet expansions for pure supercritical CO_2. We examine expansions from orifices rather than capillary tubes to avoid heat transfer and viscous effects [6].

THEORY AND NUMERICAL CALCULATIONS

Figure 1A is a shadowgraph, discussed below, of a supercritical CO_2 expansion from a 90 micron orifice impacting a flat plate, showing the shock structure. Figure 1B is a calculated density contour, discussed below, of a similar expansion. The fluid flows from a reservoir at stagnation temperature T_o and pressure P_o through a sharp-edged orifice into atmosphere. The fluid accelerates very rapidly to sonic conditions at the orifice (Mach number M=1), and then even more rapidly in the supersonic free-jet expansion, which is terminated by shock waves on the sides (barrel shocks) and the centerline (mach disk) where the flow rapidly adjusts pressure and temperature, and becomes subsonic. The flow then dissipates into atmosphere or is directed at a flat plate. Because of the rapid flow rate we neglect viscosity and heat transfer effects for the expansion. Neglecting chemical reactions, which includes condensation, the flow is then reversible and isentropic, until the non-isentropic shock waves occur.

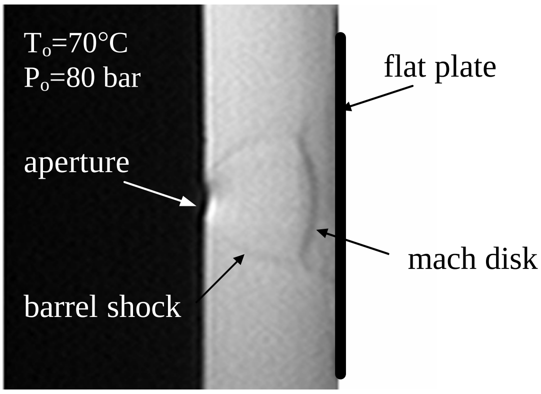

Figure 1A: CO_2 Free-Jet Shadowgraph

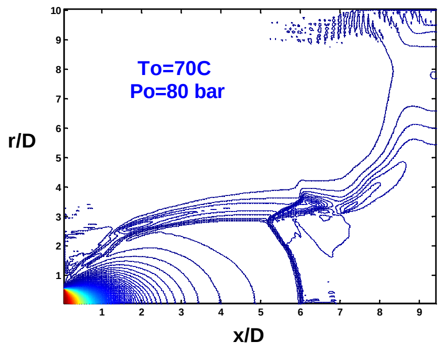

Figure 1B: CO_2 Computed Density Profiles

The time dependent partial differential equations to be solved for the axisymmetric free-jet (ASFJ) supersonic expansion, starting at M=1 at the orifice exit, are well established [11] and are of the form given in equation (1). An approximation to the two dimensional flow field are the quasi-one dimensional equations (QOD), represented by equation (2).

$$\frac{\partial e}{\partial t} + \frac{\partial f}{\partial x} + \frac{\partial g}{\partial r} + \frac{h}{r} = 0 \qquad (1)$$

$$\frac{\partial e}{\partial t} + \frac{\partial f}{\partial x} = J \qquad (2)$$

The column vectors **e**, **f**, **g**, and **h**, and **J**, have elements for mass, momentum, and energy. For example, for the ASFJ, **e** is a column vector with elements ?, ?u, ?v, and ?(E + ½(u^2 +v^2)) for mass, x and r momentum, and energy. The QOD equations are often used in compressible flow to study subsonic-to-supersonic expansions in nozzles where a physical nozzle area A(x) is prescribed [8,12]. For example, in the QOD approximation the **e** elements in equation (2) are ?A, ?Au, and ?A(E + ½u^2) [11]. The equations are quasi-one dimensional because the properties are assumed to change only in the flow coordinate x along the nozzle centerline, and to be constant normal to this direction. The QOD equations are obtained rigorously from the exact axisymmetric equations by integrating over the direction normal to the centerline. Unfortunately the free-jet has no nozzle boundary so the area A(x) is not prescribed. However, a common approach is to solve the ASFJ problem for Mach number along the centerline, and then use these rigorous results to work backwards with the QOD equations to identify an effective A(x) which will mimic the ASFJ. For our QOD studies we have taken an A(x) which closely mimics the ideal gas with constant specific heat ratio ? =1.4 expansions; our results below suggest that this is a reasonable ideal gas approximation. The QOD calculations can also be easily extended into the subsonic regime upstream of the sonic exit. We obtained an A(x) approximation for this regime based on early pitot tube data for real nozzles [9]. At steady state, the QOD equations can be integrated and become five algebraic equations in five unknowns, which can be solved exactly, providing a test for the numerical solution of the time dependent equations. We use the QOD results to compare equations of state, to test our time marching numerical calculation, and to make preliminary assessments of kinetic effects, such as vibrational relaxation [12].

The details of our ASFJ numerical calculations will be published elsewhere. We used a Lax-Wendroff two step, corrector-predictor method, with numerical viscosity [10,11]. A rectangular 240x226 grid was used with standard boundary conditions, involving symmetry or mirror reflections and outflow conditions with gradients set equal to zero. To be complete, equations (1) and (2) require thermodynamic equations of state, P(?,T), E(?,T), s(?,T), which we take from standard texts [13]. We also examined vibrational relaxation [8,12] for the degenerate $?_{2,3}$ modes of CO_2, using the QOD expansion, and found that vibrational energy has negligible contribution to the expansion beyond the sonic exit, so that a reasonable ideal gas approximation for CO_2 is expected to be constant ? =1.4.

Table 1: Quasi-One Dimensional Calculations

		at throat	**before shock**	**after shock**
Pressure P/P_o	Exact RK	.54	.00025	.012
	Lax-Wendroff RK	.56	.00025	.011
	Exact PR	.57	.00024	.012
	Lax-Wendroff PR	.55	.00024	.012
	Exact IG	.53	.00020	.012
	Lax-Wendroff IG	.53	.00024	.011
Temperature T/T_o	Exact RK	.83	.088	.74
	Lax-Wendroff RK	.86	.090	.69
	Exact PR	.86	.084	.72
	Lax-Wendroff PR	.85	.083	.66
	Exact IG	.83	.088	.97
	Lax-Wendroff IG	.84	.080	.92

Table 1 gives QOD results for expansion of CO_2 at 70^{o}C and 80 bar into atmosphere, in a prescribed converging-diverging nozzle A(x), as described above. A shock wave exists near the nozzle exit so that we can compare results across the shock. Table 1 compares exact and time marching numerical solutions of the QOD equations at three positions, using Redlich-Kwong (RK), Peng Robinson (PR), and (? =1.4) ideal gas (IG) equations of state. The sonic condition occurs at the throat and determines the mass flow rate. These results show that the time marching calculation works well but is least reliable downstream of the shock, that both the RK and PR give similar results, and that the ideal gas approximation is poorest for temperature after the shock. We report only RK and IG calculations for the ASFJ below.

Figure 2 shows a comparison between the QOD results for RK and IG, and experimental data for mass flow rate over a range of source pressures, for expansions through 50 and 90 micron orifices at source temperature T_o = 70°C. The RK equations do well, but the ideal gas is not acceptable.

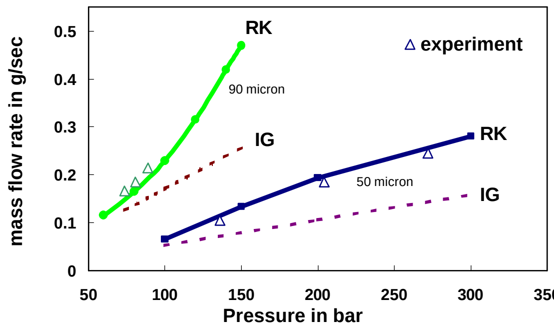

Figure 2: Calculated and Experimental Mass Flow Rate

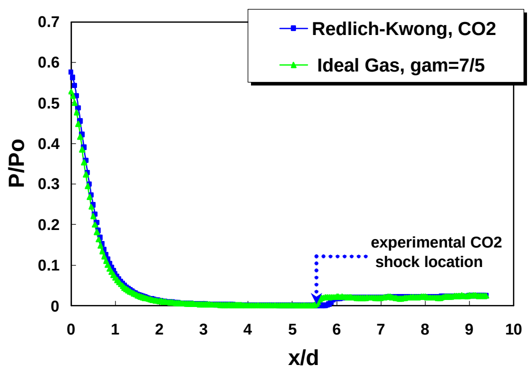

Figure3: ASFJ Centerline Pressure Profile

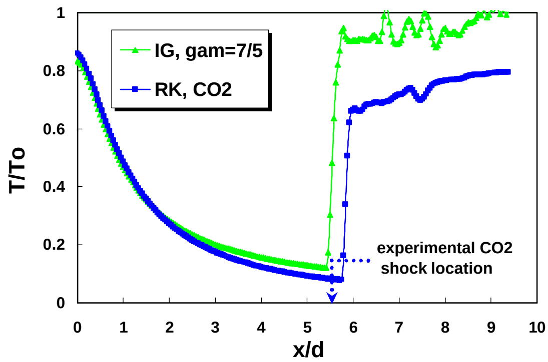

Figure 4: ASFJ Centerline Temperature Profile

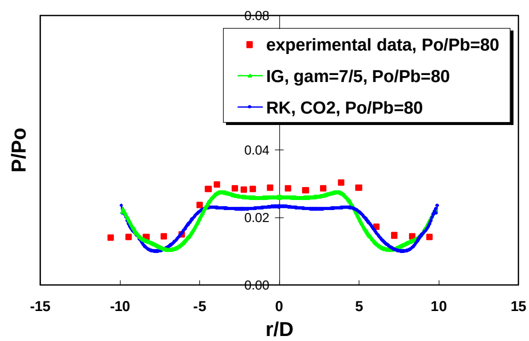

Figure 5: ASFJ Pressure Profile along Plate

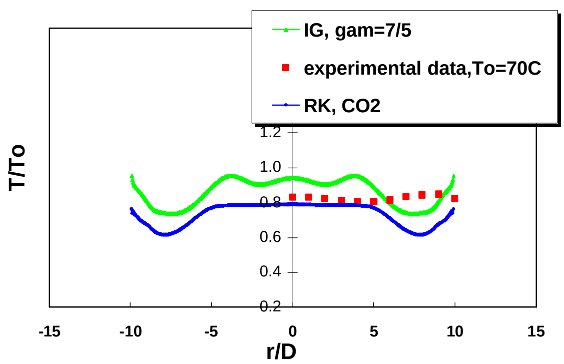

Figure 6: ASFJ Temperature Profile along Plate

Figure 1B shows our calculated density contours for a supercritical CO_2 ASFJ expansion , at 70°C and 80 bar, directed at a flat plate, indicating the rapid changes through the barrel and normal shock waves. The main features of the flow seen in figure 1A are reproduced quite well. Figures 3 and 4 show the ASFJ profiles for P, T, along the centerline, and figures 5 and 6 show P and T profiles along the flat plate; the experimental data are discussed below. The results demonstrate the ability of the numerical method to capture the shock waves, but with numerical downstream oscillations. The principal non-ideal gas effect is on the temperature after the shock wave. Although perhaps fortuitous, in light of the mass flow results, the ideal gas calculation appears to be a useful approximation for the expansion upstream of the shock and at the plate.

EXPERIMENTS AND COMPARISON WITH THEORY

The CO_2 delivery system was standard using an ISCO pump and Omega strain gauge pressure transducers. The small nozzle orifices were made from microscope apertures welded into stainless steel swagelok fittings. The nozzles were mounted into a small stainless steal block with a thermocouple inserted directly into the stagnation chamber, just upstream of the aperture. The CO_2 was preheated in a water bath and then controlled by a small resistive heater in the nozzle block assembly. Nozzle diameters were calibrated in-situ by measuring the flow rates for ideal gas Ar expansions. All source conditions were above the critical point, and for which both the entropy and the specific volume exceeded the critical point values throughout the expansion.

The shadowgraph method [14] used a lamp light source, a 10 cm diameter planar-convex lens, and a Nikon camera with a 28-108 mm zoom lens with a maximum f/3.5 aperture. The technique is sensitive to the spatial second derivative of density, and a typical photo is shown in figure 1A. From this photo the position $(x/D)_{MD}$ of the Mach disk shock waves can be measured to within 0.25 orifice diameters. To verify the accuracy of our measurements, we compare results for the Mach disk location for Ar expansions into atmosphere, no plate, with well established ideal gas results in figure 7. The Mach disc location for ideal gases is insensitive to the specific heat ratio and given by $(x/D)_{MD} = 0.67\ (P_o/P_b)^{1/2}$, where P_b is the background ambient pressure [8,9]. Insertion of a flat plate moves the normal shock wave closer to the source. Figure 8 shows data for the shock position as a function of the plate position for CO_2, together with few numerical results. Figures 3 and 4 also show that the ASFJ numerical calculation predicts the shock wave location reasonably well with the RK equation of state. Again, the ideal gas is a useful approximation.

Pressure data on the plate was obtained by mounting the pressure transducer near the plate surface with a 100 micron aperture, to provide spatial resolution (r/D) of about 1 orifice diameter. Figure 5 shows data comparing the experiment with both the RK and the ideal gas calculations. The agreement is good at the center, and again shows that the ideal gas appears to be useful.

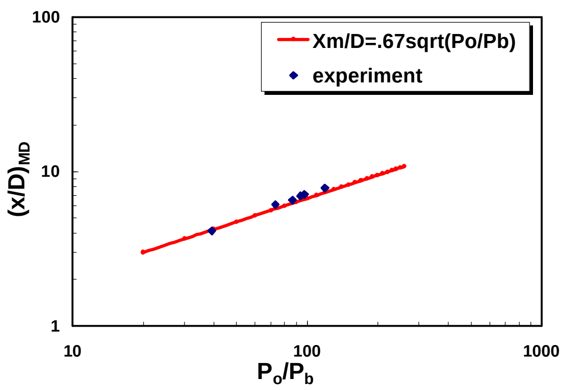

Figure 7: Mach Disk Location for Argon Free-Jet

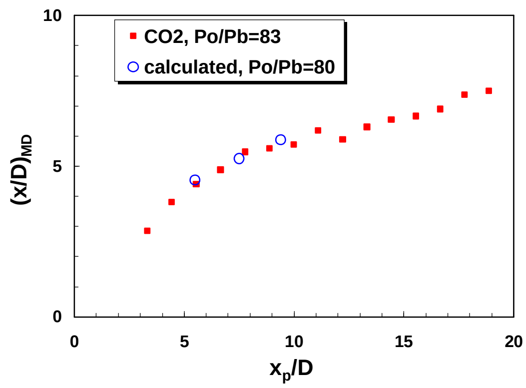

Figure 8: Mach Disk Location as a Function of Plate Distance for CO_2

Quantitative temperature measurements, both in the expansion and on the plate, are difficult because of probe heat transfer effects. We will report qualitative temperature probes of the expansion elsewhere, but figure 6 includes temperature results on the flat plate near the centerline, taken with a thermocouple placed flush with the surface; the thermocouple was too large, 250 micron, to resolve the profile. While only qualitative, we again see the usefulness of the calculations. Both the pressure and temperature plate profiles indicate a circular core of high pressure and temperature, falling off to lower values near five nozzle diameters. Often researchers have reported rings of solute deposits. The present results, when coupled to nucleation/precipitation models, may offer a useful explanation.

In conclusion, we have been able to extend time marching, compressible flow calculations to non-ideal gases, which model supercritical CO_2 RESS experiments. Since these supersonic expansions extend into the thermodynamic two-phase regimes, and we have neglected any kinetic or thermodynamic condensation considerations, it is surprising and interesting that the results seem to compare reasonable well with the experiments. Perhaps fortuitously, the ideal gas is a reasonable first approximation. We are proceeding to improve the numerical method, especially numerical viscosity, to include classical nucleation kinetics into the equations, and to add solutes to the CO_2. We will also incorporate the sources into a time-of-flight mass spectrometer molecular beam facility which will permit us to probe the free-jet expansion and identify solute clusters [7].

REFERENCES

[1] Arai, Y., *Supercritical Fluids: Molecular Interactions, Physical Properties, and New Applications*, Springer, New York, **2001**.

[2] Matson, D., Peterson, R., Smith, R., *J. Materials Science*, Vol. 22, **1987**, p. 1919.

[3] Kwauk, X., Debenedetti, P., *J. Aerosol Science*, Vol. 24, **1993**, p. 445.

[4] Brand, J., Miller, D. R., *Mat. Res. Soc.*, Vol. 131, **1989**, p. 617.

[5] Reverchon, E., Pallado, P., *J. Supercritical Fluids*, Vol. 9, **1996,** p. 216.

[6] Maharrey, S., Miller, D. R., *AIChE Journal*, Vol. 47, **2001**, p. 1203.

[7] Maharrey, S., Miller, D. R., *J. Phys. Chem. A*, Vol. 105, **2001**, p. 5860.

[8] Miller, D. R., *Free Jet Sources*, in Molecular Beam Methods, Vol. 1, G.Scoles, ed., Oxford University Press, New York, **1988**; p. 14.

[9] Ashkenas, H., Sherman, F., in *Rarefied Gas Dynamics*, Vol. 2, edited by J. Deleeuw Academic Press, New York, **1966**; p. 84.

[10] Sinha, R., Zarkay, V., Erdos, J., *AIAA Journal*, Vol. 9, **1971**, p. 2363.

[11] Anderson, J. D., *Computational Fluid Dynamics, The Basics with Applications*, McGraw-Hill, **1995**.

[12] Anderson, J. D., *AIAA Journal*, **1970**, Vol. 8, p. 545.

[13] Sandler, S. I., *Chemical and Engineering Thermodynamics*, John Wiley, **1999**.

[14] Liepman, H. W., Puckett, A. E., *Introduction to Aerodynamics of a Compressible Fluid*, John Wiley, New York, **1947**.